Proc. Natl. Acad. Sci. USA
Vol. 94, pp. 6228–6231, June 1997
Cell Biology

Assembly and positioning of microtubule asters in microfabricated chambers

(centrosome/microtubule-organizing center/centering/polymerization force)

TIMOTHY E. HOLY*, MARILEEN DOGTEROM†, BERNARD YURKE†, AND STANISLAS LEIBLER*‡§

Departments of ‡Molecular Biology and *Physics, Princeton University, Princeton, NJ 08544; and †Bell Laboratories, Lucent Technologies, Murray Hill, NJ 07974

Communicated by Arnold J. Levine, Princeton University, Princeton, NJ, April 11, 1997 (received for review February 28, 1997)

ABSTRACT **Intracellular organization depends on a variety of molecular assembly processes; while some of these have been studied in simplified cell-free systems, others depend on the confined geometry of cells and cannot be reconstructed using bulk techniques. To study the latter processes *in vitro*, we fabricated microscopic chambers that simulate the closed environment of cells. We used these chambers to study the positioning of microtubule asters. Microtubule assembly alone, without the action of molecular motors, is sufficient to position asters. Asters with short microtubules move toward the position expected from symmetry; however, once the microtubules become long enough to buckle, symmetry is broken. Calculations and experiments show that the bending-energy landscape has multiple minima. Microtubule dynamic instability modifies the landscape over time and allows asters to explore otherwise inaccessible configurations.**

Molecular assembly in eukaryotic cells is physically constrained to dimensions of typically a few (tens of) micrometers. On these length scales, microstructures can be readily fabricated by using photolithography and etching techniques, allowing for the *in vitro* study of processes in which physical constraints play a crucial role. One such process is the positioning of microtubule asters during fertilization (1, 2), mitosis (3, 4), and interphase (5–7). *In vivo* studies suggest that asters position themselves as a consequence of microtubule polymerization (5, 6) or the action of molecular motors (4, 8). To single out the role of microtubule polymerization, we set up an *in vitro* system using microstructures that mimic the geometry of cells.

MATERIALS AND METHODS

Microfabrication. Chromium (150 Å thick) was evaporated onto clean coverslips. Photoresist was applied using a spin-coater, soft-baked, then exposed to UV through a mask and developed. After a hard bake, the chromium was etched away in the exposed areas, and the glass was etched in buffered hydrofluoric acid to the desired depth. The remaining resist and chromium were stripped away, and the coverslips were cleaned in ethanol.

Tubulin and Centrosome Purification. Tubulin was purified from bovine brain through two cycles of polymerization–depolymerization, followed by phosphocellulose chromatography and an additional polymerization-depolymerization cycle (9). Tubulin was labeled with rhodamine or biotin (10). Centrosomes were isolated from cultured Chinese hamster ovary (CHO) cells (11).

Artificial Microtubule-Organizing Centers (AMTOCs). Microtubules were assembled using tubulin and biotinylated tubulin (100:1 ratio) and crosslinked using 1-ethyl-3-(3-dimethylaminopropyl)carbodiimide (4 mM for 30 min) in a solution of 50% sucrose/BRB80 (80 mM K-Pipes/1 mM $MgCl_2$/1 mM EGTA, pH 6.8). The reaction was quenched by adding sodium phosphate, pH 6.8, to 0.1 M and incubating for at least 1 hr. The microtubules were sheared through a 26 gauge needle (12), then incubated with M280 streptavidin-coated superparamagnetic beads (Dynal) for 1 hr. The beads were washed several times with buffer and stored at −80°C in 50% sucrose/BRB80. At 37°C a typical AMTOC nucleates 25–45 microtubules at a tubulin concentration of 1.6 mg/ml. Although the microtubules are not polarized as in a centrosome, the difference of the assembly speed at the two ends effectively ensures that the longest microtubules are polarized.

Sample Preparation. Solutions containing various concentrations of tubulin (15% rhodamine-labeled), 1 mM GTP, an oxygen scavenging system (50 mM glucose, 0.4 mg/ml glucose oxidase, 0.2 mg/ml catalase, 4 mM dithiothreitol), and microtubule-organizing centers (MTOCs) in BRB80 (and 0.3% Triton X-100 and 2 mg/ml BSA for AMTOC experiments) were placed on glass surfaces (coverslips or slides). These surfaces were precoated with a thin layer of agarose to ensure a tight seal of the chambers. The coverslips with wells were positioned over the solutions and sealed by applying pressure [300 psi (2.07 MPa) for 2 min] while blotting excess fluid. For experiments with AMTOCs, the wells were also precoated with agarose by using a spin-coater. To prevent the MTOCs from sticking, all surfaces were preincubated with BSA or α-casein and briefly air dried. The edges of the sample were sealed with valap (1:1:1 Vaseline/parrafin/lanolin) or paraffin.

Video Microscopy and Computer Tracking. Samples were observed on an inverted microscope (Zeiss Axiovert or Nikon Diaphot) set up for epifluorescence and differential interference contrast (DIC) microscopy. The quality of the confinement (seal) was evaluated by examining the sample in fluorescence mode. Sample temperature was controlled by heating and cooling the oil-immersion objective; the temperature was set to 37°C (30°C for centrosome experiments) to polymerize microtubules and to 12°C to induce microtubule depolymerization. DIC images were recorded continuously, fluorescence images were recorded intermittently with a shutter (0.25 s of every 10 s). The image was viewed with a charge-coupled device (CCD) camera (Paultek), contrast was enhanced with an image processor (Imagen), and the signal was recorded in VHS format. The tape was converted to JPEG movie format on a Silicon Graphics workstation, and the position of the MTOC was tracked using home-written software. Contrast in the fluorescence images was further enhanced by averaging and background subtraction.

The publication costs of this article were defrayed in part by page charge payment. This article must therefore be hereby marked "*advertisement*" in accordance with 18 U.S.C. §1734 solely to indicate this fact.

Abbreviations: MTOC, microtubule-organizing center; AMTOC, artificial MTOC.

§To whom reprint requests should be addressed.

Calculations and Simulations. Microtubules were assumed to grow from the aster at fixed angles and bend when they contact the chamber edges. The equations for the bending of a rod (13) were solved, assuming no friction between the edges and the microtubules. Simulations included dynamic instability modeled by catastrophe and rescue rates, and growth and shrinking velocities (14).

RESULTS AND DISCUSSION

We fabricated wells in glass which were a few micrometers deep and a few tens of micrometers in diameter. A single glass coverslip can contain thousands of wells of different sizes and shapes. These wells were filled with solutions and then sealed to form confined three-dimensional chambers; events inside the chambers were monitored by video microscopy. We filled the chambers with the minimal ingredients needed to form asters (9): tubulin, MTOCs, GTP, and buffer components. We used purified centrosomes as the MTOC (9), and in addition we developed an AMTOC: a latex bead coated with short stabilized microtubule seeds. Since centrosomes are complex and not fully characterized (5, 15, 16), using the AMTOCs ensures that microtubule assembly is the only origin of the phenomena we observe.

A single MTOC placed inside a chamber (with a simple shape such as circular, square, etc.) is driven to its geometric center by microtubule polymerization (Fig. 1 *a* and *b*). When the microtubules are long enough to touch the chamber edges on all sides, microtubules either stop growing (Fig. 1*a*) or buckle as they polymerize further (Fig. 1*b*). [Buckling occurs when the polymerization force exceeds the force needed to bend a microtubule of a particular length (18)]. *In vivo*, centrosomes have been observed to position themselves near the geometric center of cells (1, 2, 5, 7). Our results show that polymerization alone can center MTOCs, in the absence of any motors. By analyzing microtubule buckling [the rigidity of which is known (19)], we can estimate that the polymerization of a single microtubule generates forces of at least 1 pN. This is in the range of forces generated by a single motor (20, 21).

When two asters are present in the same chamber, they interact not just with the walls of the chamber but also with each other. Asters take positions in the chamber which result from the competition between these repulsive forces (Fig. 1*d*). This demonstrates that the interdigitation of microtubules can oppose piconewton range forces. When we induce depolymerization of the microtubules, the two asters repel each other rapidly (typically velocities are 15 μm/min, essentially the speed of microtubule depolymerization). The relief of contact with the edges of the chamber allows the interdigitated microtubules to reduce strain by pushing the asters apart. In the mitotic spindle, anisotropic microtubule growth into the spindle midzone should enhance the microtubule–microtubule interactions between asters. These interactions add to the motor-based forces known to play an important role in the mitotic spindle (3), early development in *Drosophila* (22), and other systems (23, 24).

In more complex geometries, aster positioning may proceed through a more interesting sequence of events. An example is shown in Fig. 2, in which an aster grows in a dumbbell-shaped chamber. Initially, it positions itself in the geometric center of a wide square section of the chamber. It then migrates to the edge of the square, and, after an extensive pause, moves rapidly into the neck of the dumbbell. Thus in the process of aster positioning, centers of both local and global symmetry may be attained.

When the microtubules buckle, asters often move away from the geometric center of the chamber (Fig. 3*a*). This phenomenon can have two independent causes:

(*i*) For asters with a large number of microtubules, nucleated around an isotropic MTOC, symmetry is spontaneously broken, due to the nonlinear nature of the force law of buckled microtubules. The geometric center becomes an unstable point. Numerical simulations reproduce the observed behavior (Fig. 3*b*), including long periods of directed astral motion.

(*ii*) Symmetry may also be broken directly due to anisotropy of the MTOC. For anisotropic asters, buckling displaces the aster even farther from the center (Fig. 3*c*).

The bending-energy landscape may be quite complex, often showing multiple minima (Fig. 3*c*). The barriers between minima are very high compared with thermal energies. However, the dynamic instability of microtubules (9), driven by GTP hydrolysis, continually reshapes the energy landscape, thus allowing the system to "evolve" in the otherwise inaccessible parts of configuration space (14, 25, 26).

The interplay between the action of motors and the assembly of cytoskeletal fibers seems to be crucial for many cellular phenomena such as mitotic spindle morphogenesis (27) and

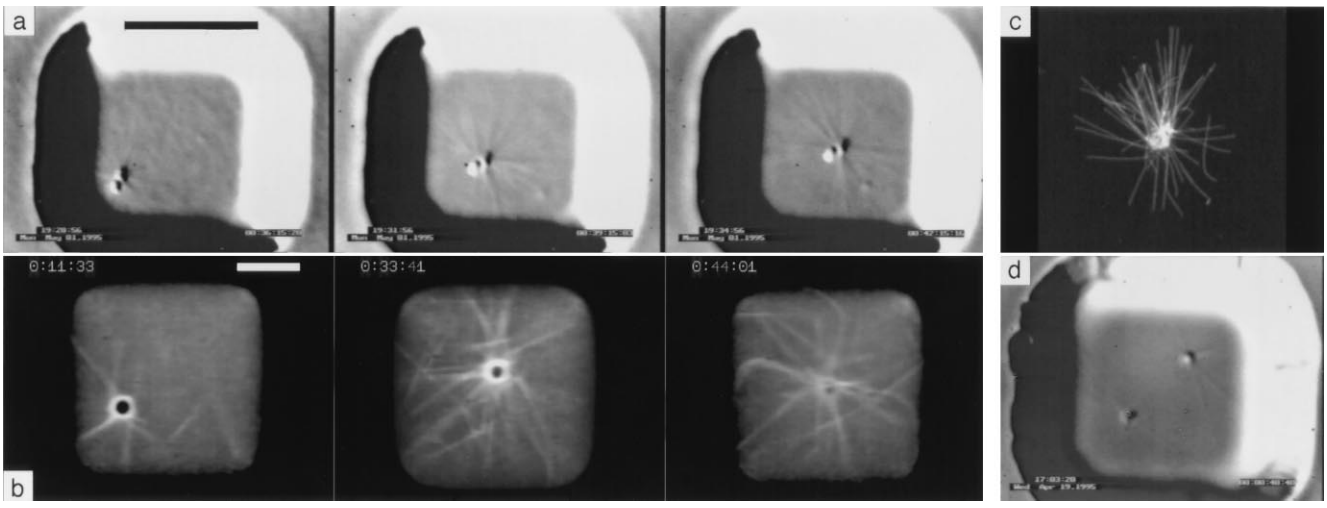

FIG. 1. Positioning of MTOCs in microfabricated chambers. (*a*) Three differential interference contrast images of a centrosome in a square chamber. The chamber is 4 μm deep and the tubulin concentration is 3.2 mg/ml. Images are 3 min apart. The slope of the well dominates the signal close to the edges of the chamber. (*b*) Three fluorescence images of an AMTOC in a square chamber. The chamber is 6 μm deep and the tubulin concentration is 1.4 mg/ml. Time is indicated in each frame. (*c*) An aster regrown from an AMTOC in 2.3 mg/ml tubulin, stabilized by diluting with 30% (vol/vol) glycerol/BRB80, spun down through a cushion of 40% glycerol/BRB80 (17) onto a coverslip coated with 3-aminopropyltriethoxysilane, and fixed with glutaraldehyde. Image taken by confocal fluorescence microscopy. (*d*) Two centrosomes in a square chamber. (All bars are 10 μm.)

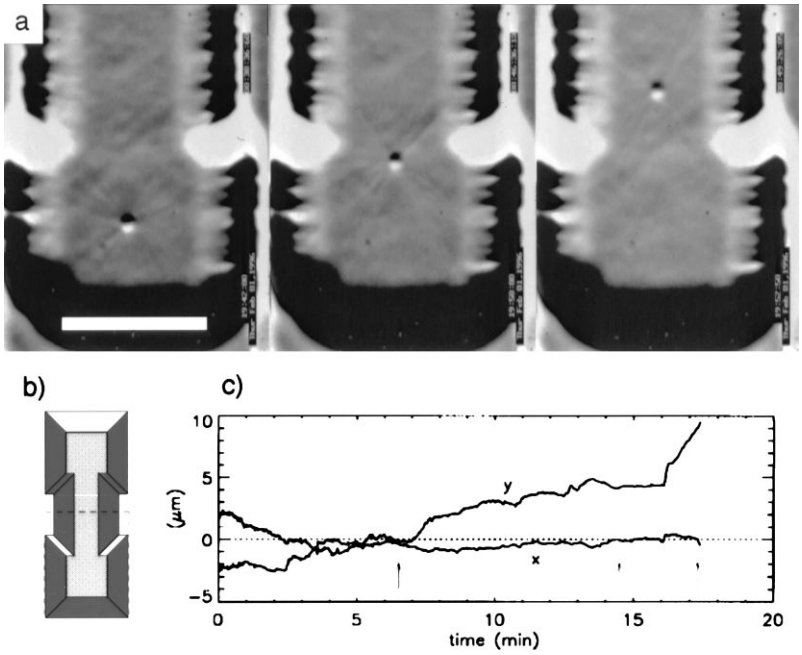

FIG. 2. (*a*) Centrosome moving in a dumbbell-shaped chamber. (Bar is 10 μm.) (*b*) Schematic view of the chamber. Only the region indicated by the broken lines is shown in *a*. (*c*) Centrosome position vs. time. The zero-line corresponds to the geometric center of the square section of the chamber. Arrows indicate the times where the images were taken.

cell locomotion (28). Experiments similar to those presented here would allow one to study this interplay under simplified conditions and to identify the contributions of each of the two sources of forces. In this paper, we have shown that microtubule polymerization alone is sufficient for aster positioning. In living cells, the barrier provided by the cell membrane is of course less rigid than our chamber walls. One would expect, however, that bending and stretching of the membrane as a result of microtubule pushing will lead to restoring forces that should cause the aster to move within the cell, allowing the aster to position itself through the same mechanism as in our *in vitro* experiments. While the counteracting forces of cytoplasmic drag are larger than in our experiments, the number of microtubules pushing against the membrane is also larger. To keep the aster positioned in the center, the cell must prevent extensive buckling of microtubules. It thus has to control microtubule length—e.g., through regulation of the parameters of dynamic instability (29, 30). As shown here, dynamic instability also provides an effective way for the aster to explore intracellular space.

Our experiments demonstrate that microfabricated sealed chambers may be used for the *in vitro* study of molecular processes for which a constrained geometry plays a central role. Their easy preparation and low cost should permit their wide use in cell biology, biochemistry and biophysics. One can imagine generalizing this approach by introducing more complex mechanical devices (valves, force transducers, etc.) or biochemical patterning of the substrate (31).

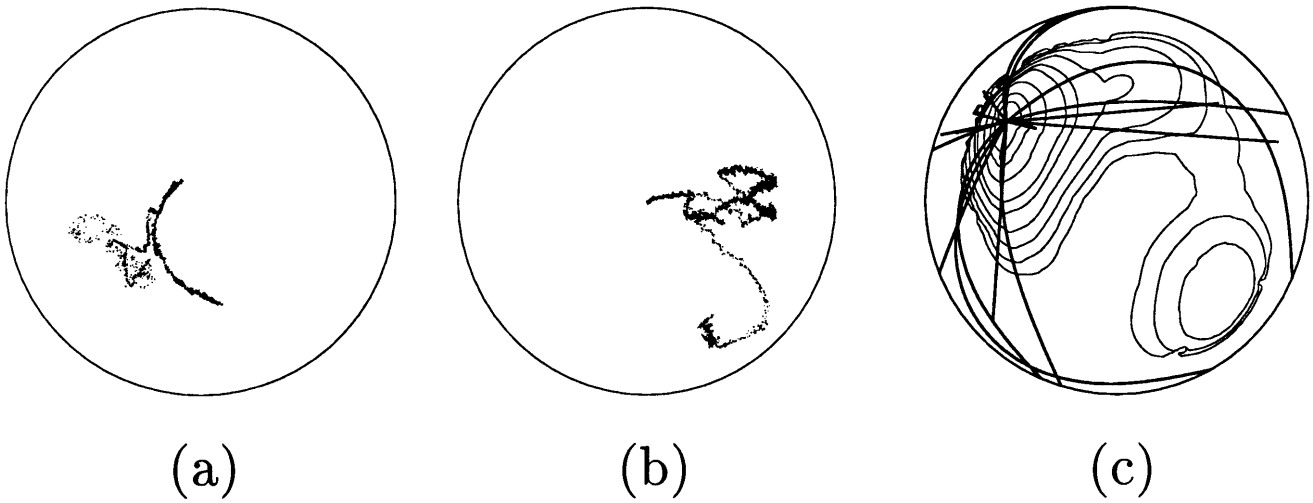

FIG. 3. Symmetry breaking in aster positioning and evolution of aster configurations. (*a*) Track of AMTOC position over a 63-min period in a 6-μm-deep circular chamber of radius 18 μm (10). The chamber edge is indicated by the circle. The tubulin concentration is 1.6 mg/ml. Each dot represents a single measurement, taken at 1-s intervals. During the interval shown here microtubules were polymerized. The longest arc was followed from the center toward the edge, increasing the displacement of the AMTOC from the center. (*b*) Track of aster position in a numerical simulation of bending and dynamic instability (24). Note the long periods of directed motion, similar to the experimental findings. (*c*) Contour plot of the total bending energy of the 20 microtubules in an aster as the position of the aster is varied (microtubule lengths and angles held constant). The aster is shown at the position of lowest energy.

We thank B. Aguera y Arcas, M. Bornens, J. Howard, E. Karsenti, A. Maggs, T. Mitchison, F. Nédélec, A. Pargellis, R. J. Smith, L. Sohn, and S.-R. Yeh for constant help, encouragement, and discussions. T.E.H. is supported by a Bell Laboratories Ph.D. Fellowship. This work was partially supported by grants from the National Institutes of Health, the National Science Foundation, and the Human Frontiers Science Project.

1. Chambers, E. L. (1939) *J. Exp. Biol.* **16,** 409–424.
2. Schatten, G. (1982) *Int. Rev. Cytol.* **79,** 59–163.
3. Ault, J. G. & Rieder, C. L. (1994) *Curr. Biol.* **6,** 41–49.
4. Karsenti, E., Boleti, H. & Vernos, I. (1996) *Cell. Dev. Biol.* **7,** 367–378.
5. Kellogg, D. R., Moritz, M. & Alberts, B. M. (1994) *Annu. Rev. Biochem.* **63,** 639–674.
6. Euteneuer, U. & Schliwa, M. (1985) *J. Cell Biol.* **101,** 96–103.
7. Euteneuer, U. & Schliwa, M. (1992) *J. Cell Biol.* **116,** 1157–1166.
8. Hamaguchi, M. S. & Hiramoto, Y. (1986) *Dev. Growth Differ.* **28,** 143–156.
9. Mitchison, T. & Kirschner, M. (1984) *Nature (London)* **312,** 237–242.
10. Hyman, A., Drechsel, D., Kellogg, D., Salser, S., Sawin, K., Steffen, P., Wordeman, L. & Mitchison, T. (1991) *Methods Enzymol.* **196,** 478–485.
11. Mitchison, T. J. & Kirschner, M. W. (1986) *Methods Enzymol.* **134,** 261–268.
12. Howard, J. & Hyman, A. A. (1993) in *Motility Assays for Motor Proteins*, Methods in Cell Biology, ed. Scholey, J. M. (Academic, San Diego), Vol. 39, pp. 105–113.
13. Landau, L. D. & Lifshitz, E. M. (1986) *Theory of Elasticity* (Pergamon, New York).
14. Holy, T. E. & Leibler, S. (1994) *Proc. Natl. Acad. Sci. USA* **91,** 5682–5685.
15. Joshi, H. C. (1994) *Curr. Opin. Cell Biol.* **6,** 54–62.
16. Snyder, M. (1994) *Chromosoma* **103,** 369–380.
17. Sawin, K. E. & Mitchison, T. J. (1991) *J. Cell Biol.* **112,** 925–940.
18. Elbaum, M., Fygenson, D. K. & Libchaber, A. (1996) *Phys. Rev. Lett.* **76,** 4078–4081.
19. Mickey, B. & Howard, J. (1995) *J. Cell Biol.* **130,** 909–916.
20. Hunt, A. J., Gittes, F. & Howard, J. (1994) *Biophys. J.* **67,** 766–781.
21. Svoboda, K. & Block, S. M. (1994) *Cell* **77,** 773–784.
22. Karr, T. L. & Alberts, B. M. (1986) *J. Cell Biol.* **102,** 1494–1509.
23. Mazia, D. (1987) *Int. Rev. Cytol.* **100,** 49–92.
24. Palazzo, R. E., Vaisberg, E., Cole, R. W. & Rieder, C. L. (1992) *Science* **256,** 219–221.
25. Kirschner, M. & Mitchison, T. (1986) *Cell* **45,** 329–342.
26. Kirschner, M. (1992) in *Molds, Molecules, and Metazoa: Growing Points in Evolutionary Biology*, eds. Grant, P. S. & Horn, H. S. (Princeton Univ. Press, Princeton, NJ), pp. 99–126.
27. Heald, R., Tournebize, R., Blank, T., Sandaltzopoulos, R., Becker, P., Hyman, A. & Karsenti, E. (1996) *Nature (London)* **382,** 420–425.
28. Mitchison, T. J. & Cramer, L. P. (1996) *Cell* **84,** 371–379.
29. Belmont, L. D., Hyman, A. A., Sawin, K. E. & Mitchison, T. J. (1990) *Cell* **62,** 579–589.
30. Verde, F., Dogterom, M., Stelzer, E., Karsenti, E. & Leibler, S. (1992) *J. Cell Biol.* **118,** 1097–1108.
31. Dogterom, M., Félix, M. A., Guet, C. C. & Leibler, S. (1996) *J. Cell Biol.* **133,** 125–140.